Available online at www.sciencedirect.com
ScienceDirect
Journal of Sound and Vibration 310 (2008) 149–168
JOURNAL OF SOUND AND VIBRATION
www.elsevier.com/locate/jsvi

Objective evaluation of interior sound quality in passenger cars during acceleration

Sang-Kwon Lee*

Acoustics Vibration Signal Processing Laboratory, Department of Mechanical Engineering, Inha University, 253 Yonghyun Dong, Inchon 402-751, Korea

Received 10 August 2006; received in revised form 11 May 2007; accepted 28 July 2007
Available online 20 September 2007

Abstract

While driving a passenger car, a driver can hear many sorts of sounds inside the car. Among them, the booming and rumbling sounds are classified as the dominant sound characteristics of passenger cars. A sound quality index evaluating the quality of these two sounds objectively is therefore required and is developed by using an artificial neural network (ANN) in the present paper. Throughout this research, the booming sound and rumbling sound were found to be effectively related to the loudness, sharpness and roughness, while the fluctuation strength is not related to these sounds. These subjective parameters are sound metrics in psychoacoustics and are used as the input of ANN. For the training process of the ANN, 150 interior sounds with booming sound quality and 150 interior sounds with rumbling sound quality of various subjective rates have been synthesized, referring to the sound characteristics of passenger cars. The other 16 interior sounds of passenger cars were obtained by measurement. The booming sound qualities and rumbling sound qualities for these interior sounds were subjectively evaluated by 21 persons for the target of the ANN. After the ANN was trained, the two outputs of this ANN were used for the booming index and rumbling index, respectively. These outputs were tested in the evaluation of the sound quality of the interior sounds which were measured inside of the 16 passenger cars. The preference rate for the 30 passenger cars was evaluated by using these two developed sound indexes. These indexes were also successfully applied to the enhancement of the interior sound quality for a developmental passenger car.

1. Introduction

Noise control in automotive engineering has long been important, but recently, a strategy for developing sound quality has also become increasingly important as a part of vehicle design. This is evidenced by the many research papers on sound quality for passenger cars that have been published in the last two decades [1–12]. As shown in Fig. 1, there are many different sound qualities inside of a car. During acceleration it is difficult to discriminate and evaluate these sounds objectively since these sounds are mixed. Passengers are able to discriminate these different sound qualities with their delicate auditory system and complex neuron structure [13]. Passengers can subjectively also evaluate each sound quality based on their sensibility. Among these sound qualities, booming sound quality and rumbling sound quality have been popularly researched

*Tel.: +82 032 860 7305; fax: +82 032 868 1716.
E-mail address: sangkwon@inha.ac.kr

0022-460X/$ - see front matter
doi:10.1016/j.jsv.2007.07.073

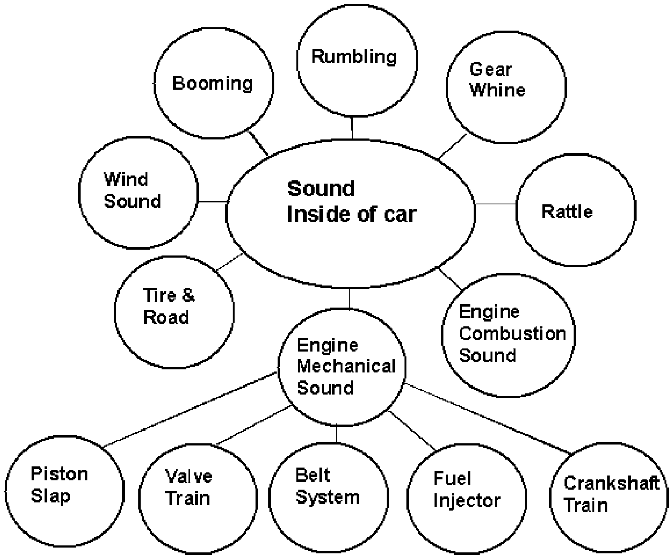

Fig. 1. Sound qualities in the compartment of a passenger car.

[1–8]. Rumbling noise is an uncomfortable sound heard in a vehicle passenger compartment during acceleration which can be annoying to a passenger. Booming noise is an unpleasant sound caused by the high sound pressure at low frequency during acceleration. In previous research on an objective rating method for the booming sound quality, it was concluded that booming sound quality is related to the loudness of the interior sound and that rumbling sound quality is related to the principal rumble component. In the present paper, it is found that the booming sound is effectively related not only to the loudness of the interior sound filtered at 200 Hz frequency by low pass filter but also sharpness, and that rumbling sound is effectively related not only to the loudness of the interior sound filtered by band pass filter with frequency band between 200 and 500 Hz but also the roughness of the interior sound. Therefore, for the loudness filtered by using a low pass filter and band pass filter, sharpness and roughness are used as the sound metrics for the development of the sound index to simultaneously evaluate the rumbling sound and booming sound of a passenger car. However, the fluctuation strength is not related to these sounds since both the booming sound and rumbling sound do not have the characteristics of the amplitude and frequency modulation at low frequencies. These metrics for the interior sound of a passenger car become the input data of the artificial neural network (ANN), which is an artificial model to identify the correlation between sound index and the subjective evaluation for the rumbling sound quality and booming sound quality of a passenger car. These models have been applied to many sound and vibration characterization problems. For noise control engineering, these models are applied to active noise cancellation [14,15]. For nonlinear dynamic problems [16] and system identification for active vibration control [17], these models are applied. The structure of the ANN system used throughout this paper is shown in Fig. 2. The outputs of ANN, which are the objective rate of the rumbling sound quality and booming sound quality, form the sound index for a passenger car developed throughout this study. If this objective rate has good correlation with the subjective rate of the sound quality evaluated by the passenger, the output of the ANN becomes a good sound index. In order to use the output of the ANN as the sound index, the weights of connectors of the neurons in ANN should be optimized throughout the training process. For the training process of ANN, 150 interior sounds with booming sound quality of various subjective rates were synthesized by using the characteristics of booming sound [1–4], and 150 interior sounds with rumbling sound quality of various subjective rates were synthesized by using the characteristics of rumbling sound [5–8], respectively. The booming sound quality and rumbling sound quality for these interior sounds were subjectively evaluated by 21 persons for the target of ANN. Another 16 interior sounds of passenger cars were obtained by measurement, and their sound qualities for booming sound and rumbling sound were subjectively evaluated. All cars used in this research were run from 1600 to 4500 rev/min on a normal road. These measured interior sounds were used for confirmation for the ANN being used for the sound quality index for a passenger car.

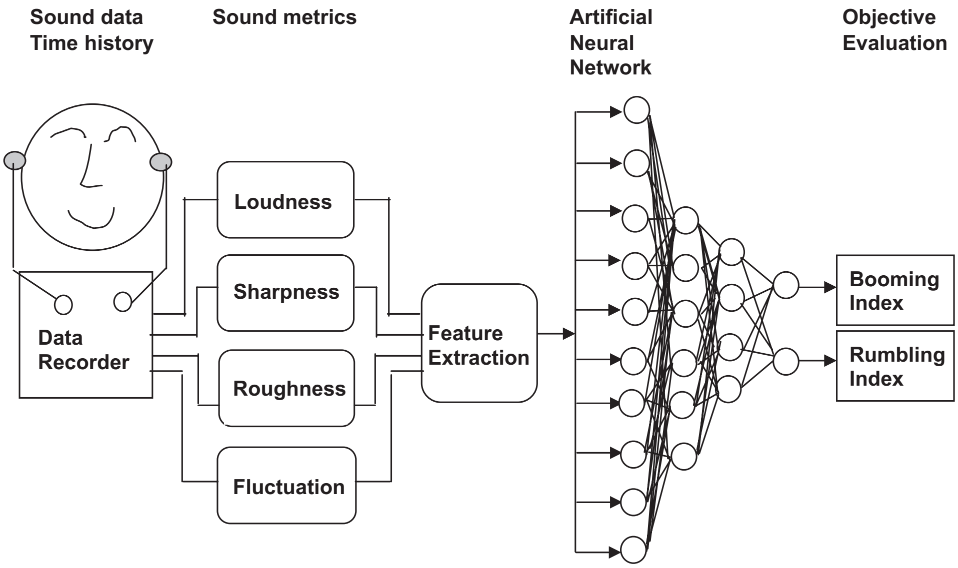

Fig. 2. Artificial neural network-based flowchart for booming index development.

Finally, the developed ANN was successfully applied to the enhancement of the interior sound quality for a developmental passenger car.

2. Artificial neural network theory

The ANN very loosely simulates a biological neural system (there is an extensive literature on the ANN [18]). A multilayer feed-forward network is used throughout this paper. The training algorithm used with this network is the back-propagation algorithm [19]. The main goal of back-propagation neural networks is the mapping of input, i.e., vector $\mathbf{x} \in R^N$ into output, i.e., vector $\mathbf{y} \in R^M$. This can be written in short as

$$x_{N\times 1} \to y_{M\times 1} \tag{1a}$$

and in general

$$x^{(p)} \to y^{(p)} \quad \text{for } p = 1, 2, \ldots, P, \tag{1b}$$

where p is the number of patterns. The mapping is performed by a network composed of processing units (neurons) and connections between them. In Fig. 3(a) a single neuron i is shown. Input signals x_j are accumulated in the neuron summing block $\sum$ and activated by function F to have only output y_i:

$$y_i = F(z_i),\ z_i = \sum_{j=1}^{N} w_{ij}x_j + b_i, \tag{2}$$

where z_i is the active potential, $w_{i,j}$ the weights of connection, b_i the threshold parameter. From among various activation functions the sigmoid functions are commonly used:

$$F(z) = \frac{1}{1+\mathrm{e}^{-\mu z}} \in (0, 1) \quad \text{for } \mu > 0, \tag{3}$$

In Fig. 3(b), a standard multiplayer network is shown. The network is composed of the input, hidden and output layers, respectively. Each neuron is connected with all neurons of the previous and subsequent layers, but there are no connections inside the layer. An example of the network, shown in Fig. 3(b), is of 4–5–3–2 structure, i.e., there are $N = 4$ inputs; $H_1 = 5$, $H_2 = 3$ are numbers of neurons in two hidden layers, and the output layer has $M = 2$ outputs. The weights $w^l_{i,j}$ and biases b^l_i (where l is the number of the layer) are called the *network parameters*. The values of the network parameters are computed iteratively in the process of

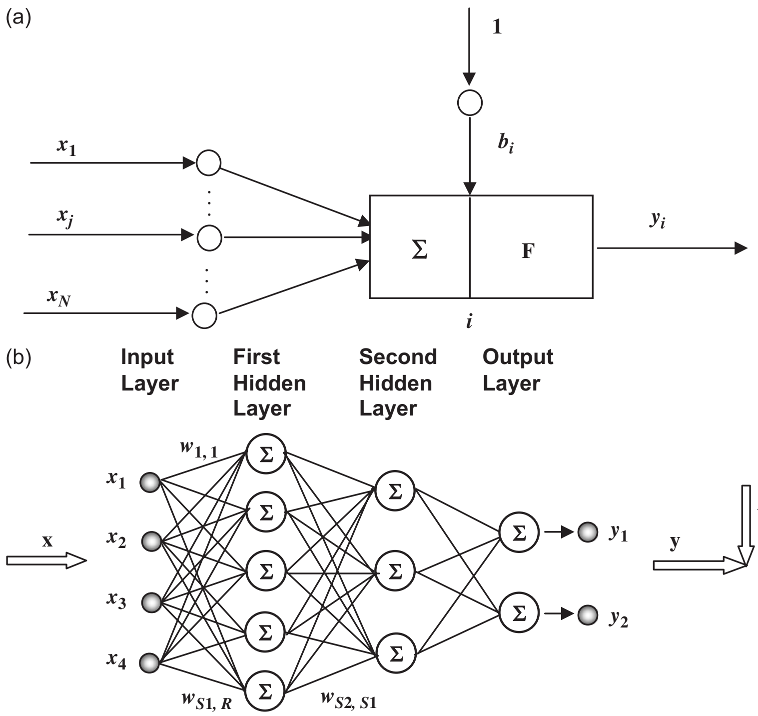

Fig. 3. Structure of artificial neural network for booming index: (a) single neuron I and (b) three-layer, back-propagation network.

network training (learning). After training, the network should be tested. That is why a set of patterns $\mathscr{P}$, composed of the pairs of known input and output vectors, is formulated (or selected from space $\mathscr{R}$ in which certain rules are obeyed):

$$\mathscr{P} = \left\{ (\mathscr{X}, t)^{(p)} \middle| p = 1, ..., P \right\} \subset \mathscr{R}, \tag{4}$$

where $x^{(p)}$, $t^{(p)}$ is the input and target vectors for the pth pattern and P the number of patterns. From the set P the training and testing sets, L and T, respectively, are selected:

$$\begin{aligned} \mathscr{L} &= \{(\mathscr{X}, t)^{(p)} | p = 1, \ldots, L\}, \\ \mathscr{T} &= \{(\mathscr{X}, t)^{(p)} | p = 1, \ldots, T\}. \end{aligned} \tag{5}$$

The signals $x_i^{(p)}$ are transmitted in the forward direction, i.e., from the input to output as shown Fig. 3(b). After computation, the output vector $y_i^{(p)}$ can be compared with the target vector $t_i^{(p)}$ and the sum of squares error function of the network is computed:

$$E = \frac{1}{2} \sum_{p=1}^{2} \sum_{i=1}^{M} (\varepsilon^{(p)})^2 = \frac{1}{2} ||\varepsilon||^2, \tag{6}$$

where $\varepsilon^{(p)} = (t_i^{(p)} - y_i^{(p)})$ is the error for the pth pattern and $\boldsymbol{\varepsilon}$ is a vector with elements ε^n. In the Levenberg–Marquardt algorithm, the sum of squares error function is modified by

$$\tilde{E} = \frac{1}{2} \left\| \boldsymbol{\varepsilon}(\mathbf{w}_{\text{old}}) + \mathbf{Z}(\mathbf{w}_{\text{new}} - \mathbf{w}_{\text{old}}) \right\|^2 + \lambda \| \mathbf{w}_{\text{new}} - \mathbf{w}_{\text{old}} \|^2, \tag{7}$$

where the parameter λ governs the step size. The matrix $\mathbf{Z}$ is defined by

$$\mathbf{Z}_{pi} = \frac{\partial \varepsilon^n}{\partial w_i}. \tag{8}$$

For large values of λ, the value of $||\mathbf{w}_{\text{new}} - \mathbf{w}_{\text{old}}||^2$ will tend to be small. If we minimize the modified error Eq. (7), with respect to $\mathbf{w}_{\text{new}}$, we obtain

$$\mathbf{w}_{\text{new}} = \mathbf{w}_{\text{old}} - (\mathbf{Z}^{\text{T}}\mathbf{Z} + \lambda\mathbf{I})^{-1}\mathbf{Z}^{\text{T}}\boldsymbol{\varepsilon}(\mathbf{w}_{\text{old}}), \tag{9}$$

where $\mathbf{I}$ is the unit matrix. For very small values of the parameter λ we recover the Newton formula, while for large values of λ we recover the standard gradient decent. One common approach for setting λ is to begin with some arbitrary value such as $\lambda = 0.1$. The author of this paper applied the Levenberg–Marquardt learning method [19].

3. Synthetic booming sound

The interior sound of a passenger car consists of very complex frequency spectra since it has many excitation sources, resonance systems and parts of sound radiation [20,21]. However, it is known that the firing frequency component of the interior sound influences the booming sound quality [1–4]. Other frequency components play the role of background noise. For example, the firing frequency component of the interior sound of a car loaded with an in-line 4-cylinder engine is twice the rotating speed of the crankshaft of the engine. For a V6 engine, the firing frequency is three times the rotating speed of the crankshaft. Therefore, it is inferred that the booming sound quality of a passenger car is related to the amplitude change of the sound at the firing frequency. Fig. 4(a) shows a waterfall analysis for the sound pressure inside of a car loaded with an in-line 4-cylinder engine. The speed of the engine increases from 1600 to 4500 rev/min. In the figure, the

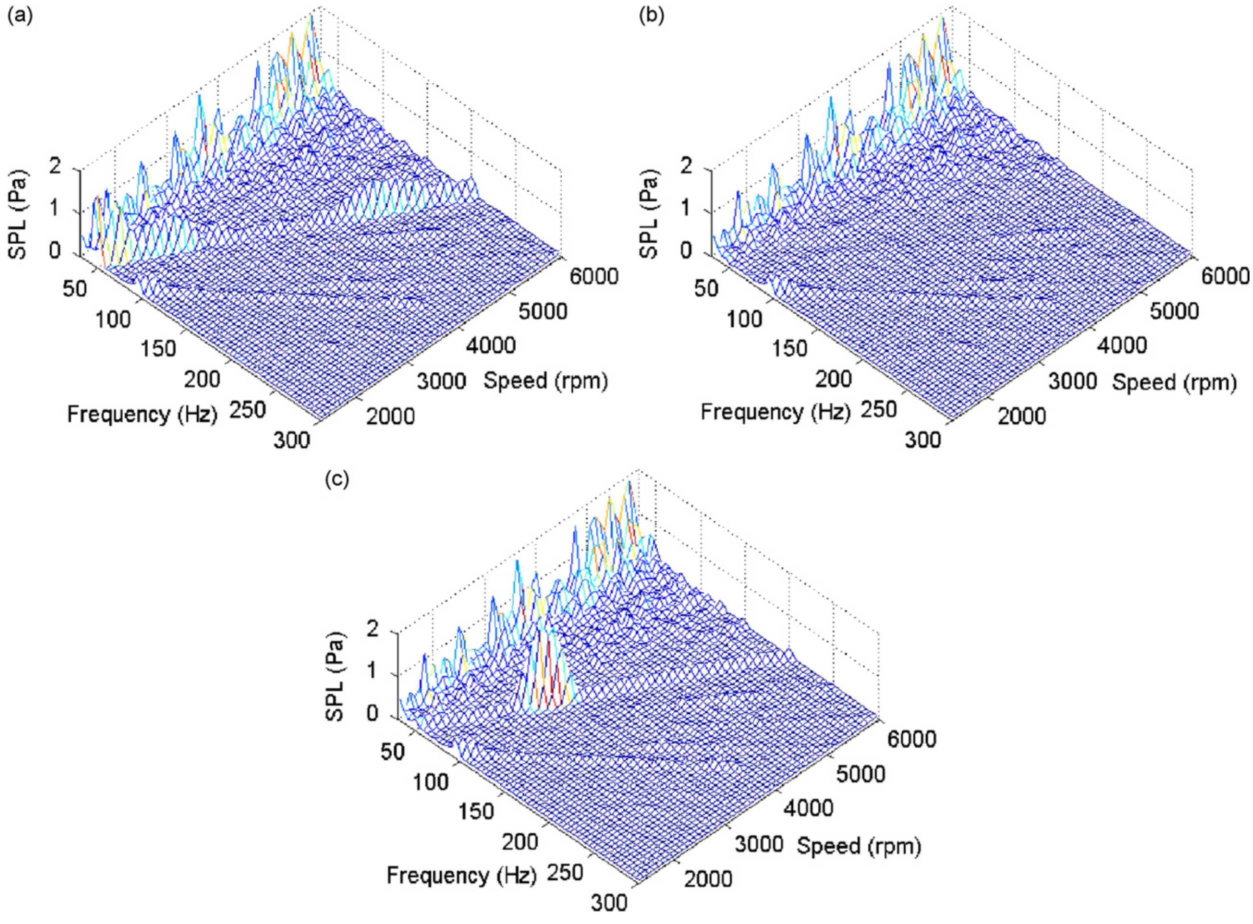

Fig. 4. Waterfall analysis for interior sound of a passenger car loaded with an in-line 4-cylinder engine: (a) base sound, (b) without firing component sound and (c) modified sound.

horizontal axis designates the frequency and the vertical axis shows the sound pressure level inside of the car. From this figure, we can see that the pressure level of the sound at the firing frequency is dominant and the firing frequency is related to the rotating speed of the crankshaft (i.e., rev/min). So if we change the amplitude of this frequency component, the booming sound quality for the interior sound of this car will also be influenced. Mathematically, the time history of this component can be expressed as an analytic signal [20,21] with the amplitude- and frequency-modulated signal as follows:

$$x(t) = a(t)e^{j\phi(t)}, \tag{10}$$

where $a(t)$ is the function associated with amplitude modulation (i.e., it is the envelope of the signal $x(t)$), and $\phi(t)$ is the function associated with frequency modulation. Fig. 5(a) represents the time history of the firing frequency component sound. It is obtained by filtering the interior sound as shown in Fig. 4(a) by using a Kalman order adaptive filter [20,22]. Fig. 4(b) shows the waterfall analysis of the interior sound obtained by removing the firing frequency component of the original interior sound. The signal of the sound with only firing frequency component is expressed as a form of the analytic signal explained in Eq. (10). The envelope and frequency modulation functions are $a(t)$ and $\phi(t)$, respectively. The instantaneous frequency for the analytic signal [20] is given by

$$f_i(t) = \frac{1}{2\pi}\frac{d\phi(t)}{dt}. \tag{11}$$

Therefore, if the engine speed is constant with firing frequency f_0, the function $\phi(t)$ is given by

$$\phi(t) = 2\pi f_0 t. \tag{12}$$

If the engine speed is changed with the firing frequency $f(t) = \gamma(t)'$, then the function $\phi(t)$ is written by

$$\phi(t) = 2\pi\gamma(t). \tag{13}$$

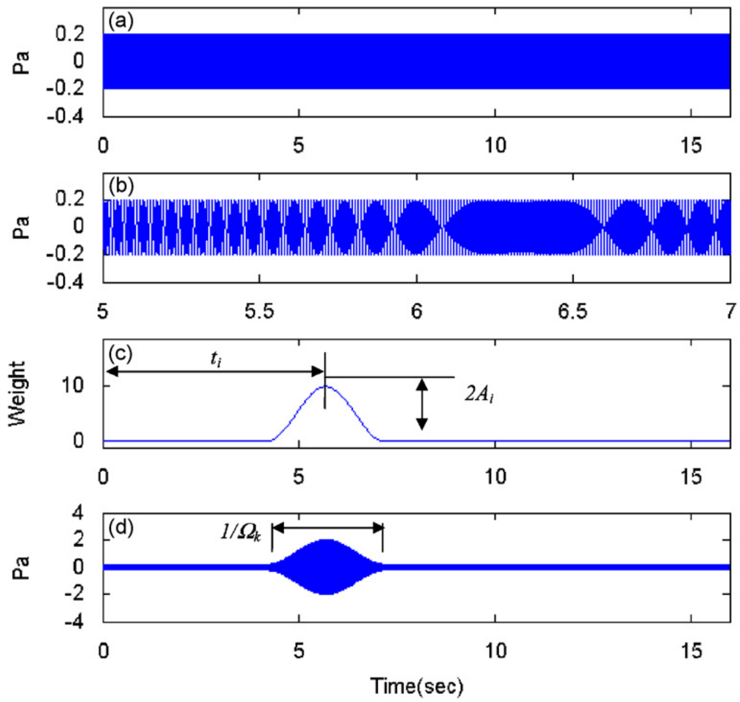

Fig. 5. Modification of firing frequency component sound for production of the 200 interior sounds: (a) base firing component sound signal, (b) Zoomed firing component sound signal, (c) design of the envelope weighting function and (d) modified base firing component sound signal with booming sound quality.

Table 1
Parameters used for production of the synthetic booming sound

Time shift t_i (center frequency)	Amplitude step A_j (decibel reference $= 2\times10^{-5}$)	Duration $T_i = 1/\Omega_k$ (frequency Ω_k)
1 s (55 Hz)	90 dB	1.54 s (0.65 Hz)
2.6 s (70 Hz)	95 dB	2.06 s (0.49 Hz)
4.1 s (85 Hz)	100 dB	3.09 s (0.32 Hz)
5.7 s (100 Hz)	105 dB	4.12 s (0.24 Hz)
7.2 s (115 Hz)	110 dB	
8.8 s (130 Hz)		
10.3 s (145 Hz)		
11.9 s (160 Hz)		
13.4 s (175 Hz)		
15 s (190 Hz)		

We can produce interior sounds with booming sound qualities of various subjective rates by modifying the envelope of the signal as shown in Fig. 5(a) and adding it to the background noise as shown in Fig. 4(b), because the background noise influences the booming sound quality. In this paper, the envelope of the analytic signal is modified as follows:

$$\begin{cases} \mathscr{A}(t) = \left[A_j \sin \Omega_k (t - t_i) + A_j + 1\right] a(t), & t_i - \dfrac{1}{2\Omega_k} \leqslant t \leqslant t_i + \dfrac{1}{2\Omega_k}, \quad i = 1 \ldots 10,\ j = 1 \ldots 5, \text{ and } k = 1 \ldots 4, \\ \mathscr{A}(t) = 1 \cdot a(t), & \text{otherwise,} \end{cases} \tag{14}$$

where $a(t)$ is the envelope of the firing frequency component of the analytic signal; t_i is the ith time where the amplitude modulation takes place; A_j is the jth magnitude for presenting the magnitude of amplitude modulation; and Ω_k represents the kth frequency for determining the duration of amplitude modulations. Table 1 presents the various values for the parameters Ω_k, t_i, and A_j used throughout this paper. Fig. 5(c) shows one example of the modified envelopes $A(t)$ and illustrates the roles of the parameters. Fig. 5(d) displays the analytic signal $x(t)$ modified by using the modified envelopes $A(t)$. The modified analytic signal is given by

$$x(t) = \mathscr{A}(t)\exp(\mathrm{j}\phi(t)). \tag{15}$$

In order to get the synthetic interior sounds with different booming sound quality, these modified analytic signals with various values for the Ω_k, t_i and A_j are added to the background noise as shown in Fig. 4(b). Fig. 4(c) shows the waterfall analysis for the synthetic interior sound using the modified analytic signal as shown in Fig. 5. With this method, the 200 synthetic interior sounds with booming sound quality of various subjective rates are completed. Among 200 synthetic interior sounds, only 150 synthetic interior sounds are used for the training of ANN. The other 50 interior sounds were removed because they are not booming-like sound but too much loud sound. The sound pressure level of these 50 interior sounds is over 110 dBA. The sound pressure level in most real passenger cars is not over 110 dBA. The subjective rates of these interior sounds are used for the target of the ANN.

4. Synthetic sound for rumbling sound quality

There are many research results on the rumbling sound quality [5–8,23]. According to these results, the sound wave formed by three continuous half-order components of the engine revolution is related to the rumbling sound quality. Fig. 6(a) shows the sound wave formed by three half-order components of engine revolution at constant speed. The sound wave is the only amplitude-modulated signal and has severe rumbling sound quality. The spectrum of this sound wave is shown in Fig. 6(b). In general, the degree of the rumbling sound quality is related to the magnitude of the envelope, the modulation frequency and the carrier frequency of the sound wave. The magnitude of the envelope of the sound wave is called the principal rumble component, which is calculated by taking the Fourier transform for the envelope of the sound wave as shown

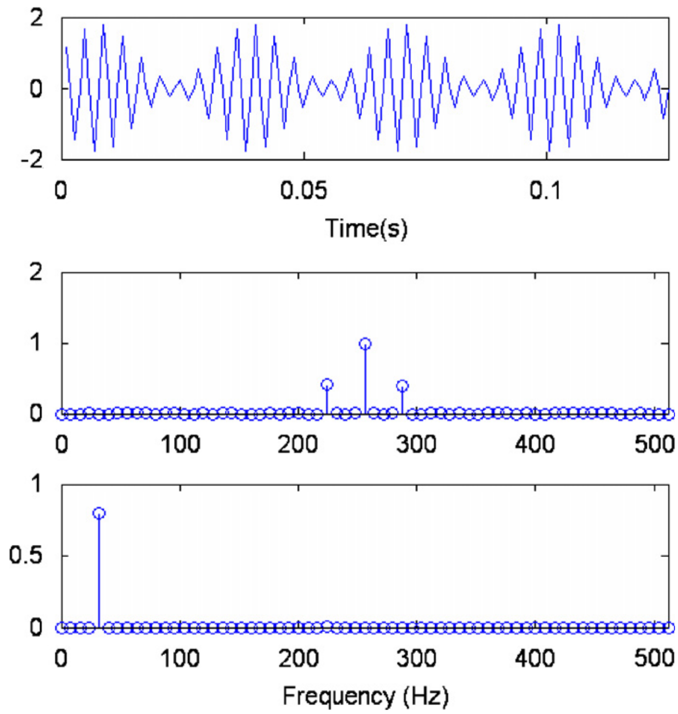

Fig. 6. Synthetic sound waves with rumbling sound quality (a) amplitude-modulated wave formed by three half-order components used for the production of a rumbling sound quality, (b) spectrum of the amplitude-modulated wave and (c) principal rumble component of the amplitude-modulated wave.

in Fig. 6(c). In this case, only one spike exists at the modulation frequency of 32 Hz since the sound wave has one amplitude-modulated signal. The frequency of the envelope of the sound wave is the modulation frequency, which is the frequency difference Δf as shown in Fig. 6(b). The range of the modulation frequency for rumbling sound is between 15 and 35 Hz [23]. In a car, the modulation frequency is half-order of the engine revolution. For example, when an engine runs at 3000 rev/min the modulation frequency is 25 Hz. Therefore, the region of the occurrence of the rumbling sound quality is associated with the limit of the modulation frequency. The carrier frequency of the sound wave, which is the center frequency as shown in Fig. 6(b), should be in the region between 150 and 500 Hz [5]. When the revolution of the engine changes as shown in Fig. 7, the sound wave formed by three continuous half-order components is not the only amplitude-modulated signal any more. In this case, the time history of this sound wave becomes the amplitude-phase-modulated signal. Mathematically, this signal can be expressed by the sum of three analytic signals [20,21] as follows:

$$x(t) = a_1(t)\mathrm{e}^{\mathrm{j}\phi_1(t)} + a_2(t)\mathrm{e}^{\mathrm{j}\phi_2(t)} + a_3(t)\mathrm{e}^{\mathrm{j}\phi_3(t)} \tag{16}$$

where $a_1(t)$, $a_2(t)$ and $a_3(t)$ are the functions associated with amplitude modulation and $\phi_1(t)$, $\phi_2(t)$ and $\phi_3(t)$ are the functions associated with frequency modulation. Each term of the right side in Eq. (16) becomes one of the three half-order components. It is obtained by using a Kalman order adaptive filter [22]. The instantaneous frequency for each half-order component [20] is given by

$$\begin{cases} f_1(t) = \dfrac{1}{2\pi}\dfrac{\mathrm{d}\phi_1(t)}{\mathrm{d}t}, \\ f_2(t) = \dfrac{1}{2\pi}\dfrac{\mathrm{d}\phi_2(t)}{\mathrm{d}t}, \\ f_3(t) = \dfrac{1}{2\pi}\dfrac{\mathrm{d}\phi_3(t)}{\mathrm{d}t}. \end{cases} \tag{17}$$

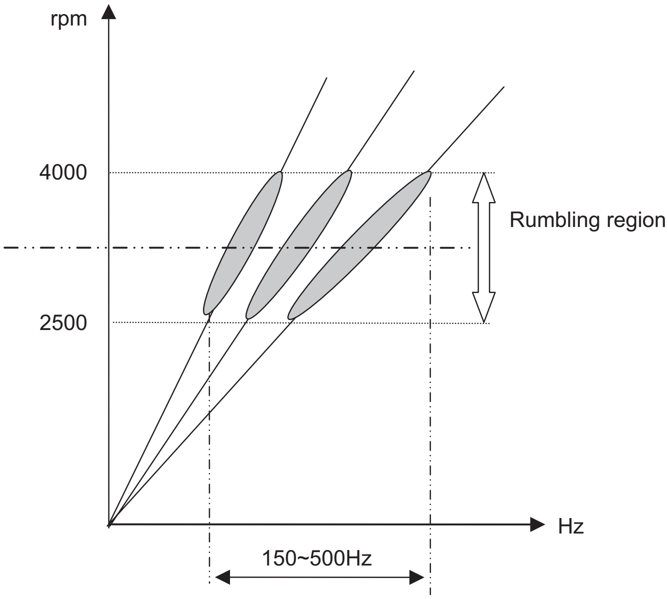

Fig. 7. Explanation for three half-order components used for the production of rumbling sound quality.

Therefore, if the engine speed is constant with frequencies f_{01}, f_{02} and f_{03}, the functions $\phi_1(t)$, $\phi_2(t)$ and $\phi_3(t)$ are given by

$$\begin{cases} \phi_1(t) = 2\pi f_{01} t, \\ \phi_2(t) = 2\pi f_{02} t, \\ \phi_3(t) = 2\pi f_{03} t. \end{cases} \tag{18}$$

If the engine speed is changed with the firing frequencies $f_1(t) = \gamma_1(t)'$, $f_2(t) = \gamma_2(t)'$ and $f_3(t) = \gamma_3(t)'$, then the functions $\phi_1(t)$, $\phi_2(t)$ and $\phi_3(t)$ are written by

$$\begin{cases} \phi_1(t) = 2\pi\gamma_1(t), \\ \phi_2(t) = 2\pi\gamma_2(t), \\ \phi_3(t) = 2\pi\gamma_3(t). \end{cases} \tag{19}$$

The degree of amplitude modulation and phase modulation of the signal $x(t)$ depends on the degree of the amplitude modulation and the phase modulation of each half-order component. We can produce interior sounds with rumbling sound qualities of various subjective rates by modifying the amplitude modulation and phase modulation of each half-order component. By replacing the original three half-order components with modified three half-order components, a new interior sound with rumbling sound quality is created. In this paper, many interior sounds with different rumbling sounds have been made by modifying the magnitude modulation and the phase modulation of each half-order component as follows:

$$\begin{cases} \mathscr{A}_1(t) = \left(B_{j,m}\cos[\Omega_k(t-t_i)-\pi] + B_{j,m} + 1\right)a_1(t) \text{ and} \\ B_{j,m} = \dfrac{r(2A_j+1)-q_m}{2q_m}, \quad t_i \leqslant t \leqslant t_i + \dfrac{2\pi}{\Omega_k} \ \ i=1,2,3,4, \ \ j=1,2,3,4,5, \ \ k=1,2,3,4, \ \ m=1,2,3, \\ \mathscr{A}_1(t) = 1\cdot a_1(t), \quad \text{otherwise}, \end{cases} \tag{20a}$$

$$\begin{cases} \mathscr{A}_2(t) = \left(A_j\cos[\Omega_k(t-t_i)-\pi] + A_j + 1,\right)\, a_2(t), \\ t_i \leqslant t \leqslant t_i + \dfrac{2\pi}{\Omega_k}, \ \ i=1,2,3,4, \ \ j=1,2,3,4,5, \ \ k=1,2,3,4, \\ \mathscr{A}_2(t) = 1\cdot a_2(t), \quad \text{otherwise}, \end{cases} \tag{20b}$$

$$\begin{cases} \mathscr{A}_{31}(t) = \left(B_{j,m}\cos[\Omega_k(t-t_i)-\pi] + B_{j,m} + 1\right)a_3(t) \text{ and} \\ B_{j,m} = \dfrac{r(2A_j+1)-q_m}{2q_m}, \quad t_i \leqslant t \leqslant t_i + \dfrac{2\pi}{\Omega_k} \; i=1,2,3,4, \; j=1,2,3,4,5, \; k=1,2,3,4, \; m=1,2,3, \\ \mathscr{A}_3(t) = 1 \cdot a_3(t), \quad \text{otherwise,} \end{cases} \tag{20c}$$

where $r = |a_2(t)/a_1(t)| = |a_2(t)/a_3(t)|$ is the ratio of the magnitude of the envelope of the middle center-order component of three half-order components to that of each side-order component, 0.0632 is used for $|a_2(t)|$,0.02 is used for $|a_1(t)|$ and $|a_3(t)|$, t_i is the ith time when the amplitude modulation occurs, A_j is the magnitude of the jth amplitude modulation as shown in Fig. 8(a), $B_{j,m}$ is the magnitude of the mth amplitude modulation of each side order for the jth carrier frequency, Ω_k represents the kth frequency for determining the duration of amplitude modulations as shown in Fig. 8(a), and q_m is the mth difference between the magnitude of the middle center-order component and the magnitudes of the side-order components of three half-order components. Table 2 presents various values for the parameters A_j, t_i, Ω_k and q_m used throughout this paper. The new wave composed of the sum of three analytic signals is given by

$$x(t) = \mathscr{A}_1(t)\exp(\mathrm{j}\phi_1(t)) + \mathscr{A}_2(t)\exp(\mathrm{j}\phi_2(t)) + \mathscr{A}_3(t)\exp(\mathrm{j}\phi_3(t)). \tag{21}$$

Fig. 8(a) shows an example of a synthetic sound wave made by using Eq. (21). Fig. 8(b) shows the zoomed version of the sound wave selected at the region where the rumbling sound occurs. The form of this sound wave is an amplitude-phase-modulated signal. The principal rumble component is calculated by taking the Fourier transform of the sound wave envelope as shown in Fig. 8(c). There are many spikes since the sound wave is an amplitude-phase-modulated signal. The principal rumble component is the magnitude of the component at the modulation frequency 28 Hz associated with half-order of the engine revolution. In order to get a number of synthetic interior sounds with different rumbling sound quality, these kinds of new waves are made by using various values for the A_j, Ω_k, t_i and q_m listed in Table 2. They should be inserted into the

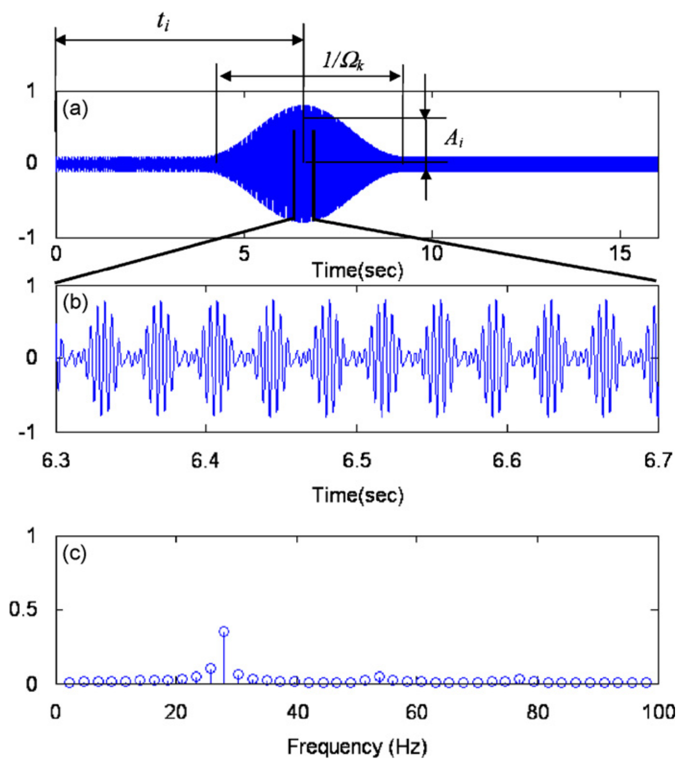

Fig. 8. Modification of three half-order components of engine revolution for production of the 240 different rumbling sounds: (a) sound wave formed by three half-order components, (b) the zoomed version of sound wave at the region where rumbling sound occurs and (c) principal rumble component of the sound wave.

Table 2
Parameters used for production of the synthetic rumbling sounds

Amplitude step A_j (decibel reference $= 2 \times 10^{-5}$)	Time shift t_i (center frequency)	Duration time $T_k = 2\pi/\Omega_k$ (frequency Ω_k)	Magnitude of modulation q_m
70 dB	3.94 s (2200 rev/min)	1.54 s (0.65 Hz)	1
75 dB	2.76 s (2500 rev/min)	2.06 s (0.49 Hz)	1.7
80 dB	4.86 s (3000 rev/min)	3.09 s (0.32 Hz)	3.16
85 dB	6.97 s (3500 rev/min)	4.12 s (0.24 Hz)	
	9.08 s (4000 rev/min)		

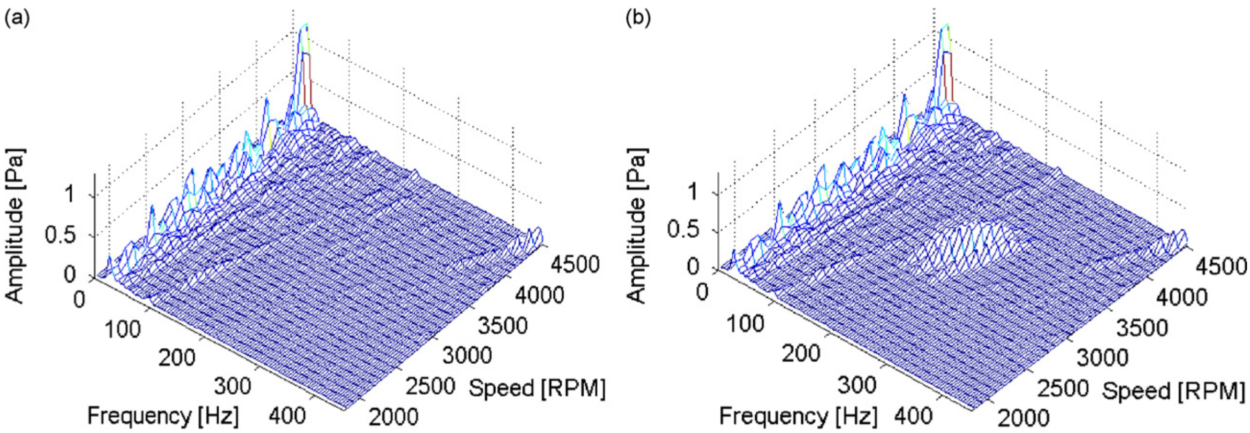

Fig. 9. Waterfall analysis for interior sound of a passenger car (a) base sound, (b) modified sound with rumbling sound quality.

background noise as shown in Fig. 9(a), which is a waterfall analysis of the signal without three half-order components. It is the interior sound measured inside of a car. Fig. 9(b) shows the waterfall analysis for a synthetic interior sound with rumbling sound. With this method, 240 synthetic interior sounds with rumbling sound quality of various subjective rates are completed. Among 240 synthetic interior sounds, only 150 synthetic interior sounds are used for the training of ANN. The other 90 interior sounds were removed because they are not rumbling-like sounds. The sound pressure level of these 90 interior sounds is over 110 dBA. The sound pressure level in most real passenger cars is not over 110 dbBA. The subjective rates of these interior sounds are used for the target of the ANN.

5. Measurement of interior sound and jury test

For the target of the ANN, the 300 synthetic interior sounds were subjectively evaluated by 21 passengers (17 males and 4 females). The 150 synthetic interior sounds are booming-like sounds. The other 150 synthetic interior sounds are rumbling-like sounds. In addition to these synthetic interior sounds, the interior sounds of 16 mass-produced passenger cars were also used for subjective evaluation. Ten vehicles out of 16 mass-product cars are passenger cars with in-line 4-cylinder engines. Four vehicles are passenger cars with V6 cylinder engines. Two vehicles are passenger cars with V8 cylinder engines. The interior sounds of the test vehicles were recorded with a binaural head system made by Head Acoustics Company in Germany. All driving tests proceeded on a normal road of the proving ground in Hyundai Motor Company in Korea. All cars were accelerated from 1800 to 4500 rev/min with wide open throttle condition. Therefore, the subjective evaluation consists of a total of 166 interior sounds for the booming sound and rumbling sound, respectively. The playback system and headphone of the Head Acoustics Company were used for subjective evaluation. The 166 interior sounds were randomly evaluated. The subjective rate was evaluated for point 4 to point 9. Table 3 illustrates the subjective rates and their relationship with the production guide of the cars.

Table 3
Grade for subjective evaluation of booming sound quality and rumbling sound quality for the interior sound of a passenger car

Subjective rates	Production guide of cars
9	Very excellent
8.5	Excellent
8	Good
7.5	Acceptable for mass production
7	Marginal
6.5	Not good
6	Bad
5.5	Unacceptable to mass production
5	Very bad
4.5	Fail (impossible to develop)

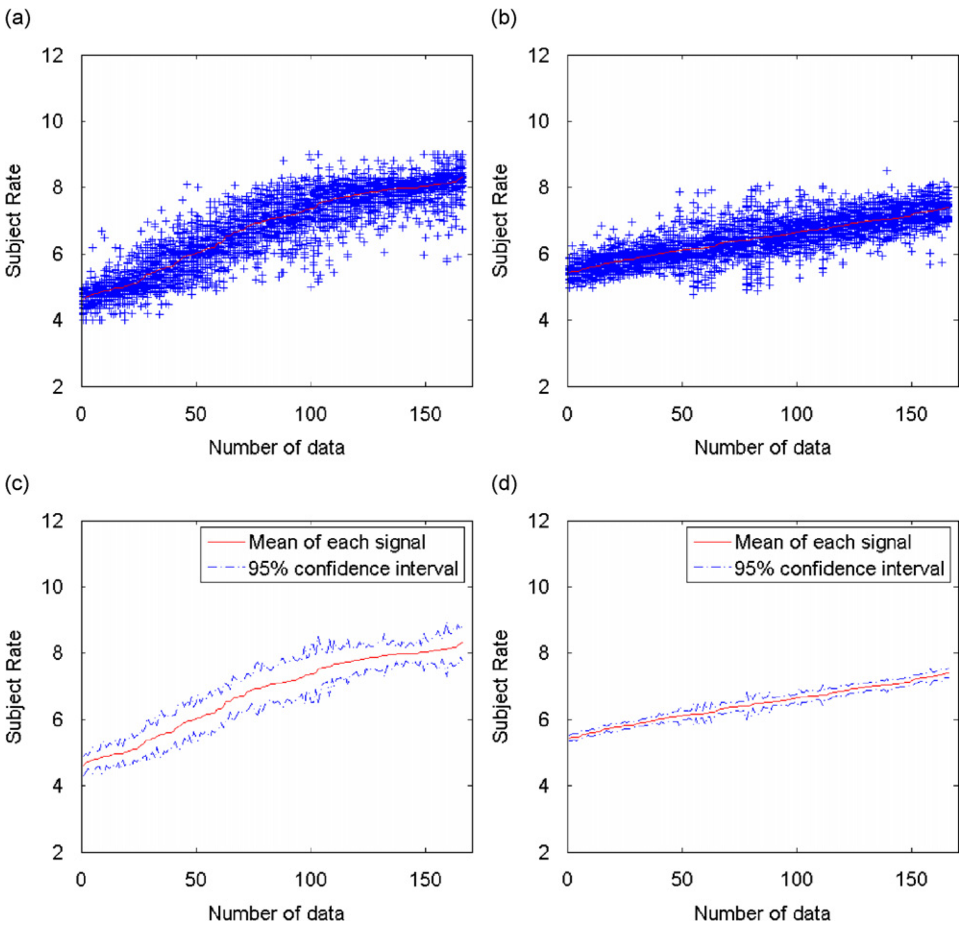

Fig. 10. Subjective rates for the 166 interior sounds of passenger cars: (a) raw subjective rate for booming sounds, (b) raw subjective rate for rumbling sounds, (c) average subjective rate for rumbling sounds and standard deviation with 95% confidence interval and (d) average subjective rate for rumbling sounds and standard deviation with 95% confidence interval.

Fig. 10 shows the results of subjective evaluation for the 166 signals. Fig. 10(a) shows the results of the subjective evaluation for the 150 synthetic booming sounds and the interior sounds measured from 16 mass-produced passenger cars. Fig. 10(b) shows the results of the subjective evaluation for the 150 synthetic rumbling sounds and the interior sounds measured from 16 mass-produced passenger cars. Fig. 10(c) and (d) show the standard deviation with a 95 percent confidence interval for each sound. It is calculated from all subjective evaluations of the car individual interior sounds. The mean values of the subjective evaluation within this deviation are used for the target of the ANN.

6. Sound metrics

In this section, the sound metrics for the 166 interior sounds are calculated for the input data of ANN. Four major sound metrics such as loudness, sharpness, roughness and fluctuation strength are discussed and these sound metrics for 166 interior sounds are shown in Figs. 11 and 12. These results are used for the input of the ANN to be used as the booming index.

6.1. Loudness

Loudness represents the auditory perception character related to the sound magnitude [13]. There are many models [13,24,25] for calculating the loudness. In this paper, the Zwicker model [13] is used for the calculation of the loudness for the 166 interior sounds. The loudness is measured in phones or sones. One sone is the loudness for pure tone sound with amplitude of 40 dB at 1 kHz. Fig. 11(a) and 12(a) show the loudness versus subjective rating for the 166 sounds for booming sound and rumbling sound, respectively. For calculation of loudness for booming sound, the 166 interior sounds are filtered at 200 Hz frequency by a low pass filter since the timbre of booming sound is a lower frequency sound [1–4]. For calculation of loudness for rumbling

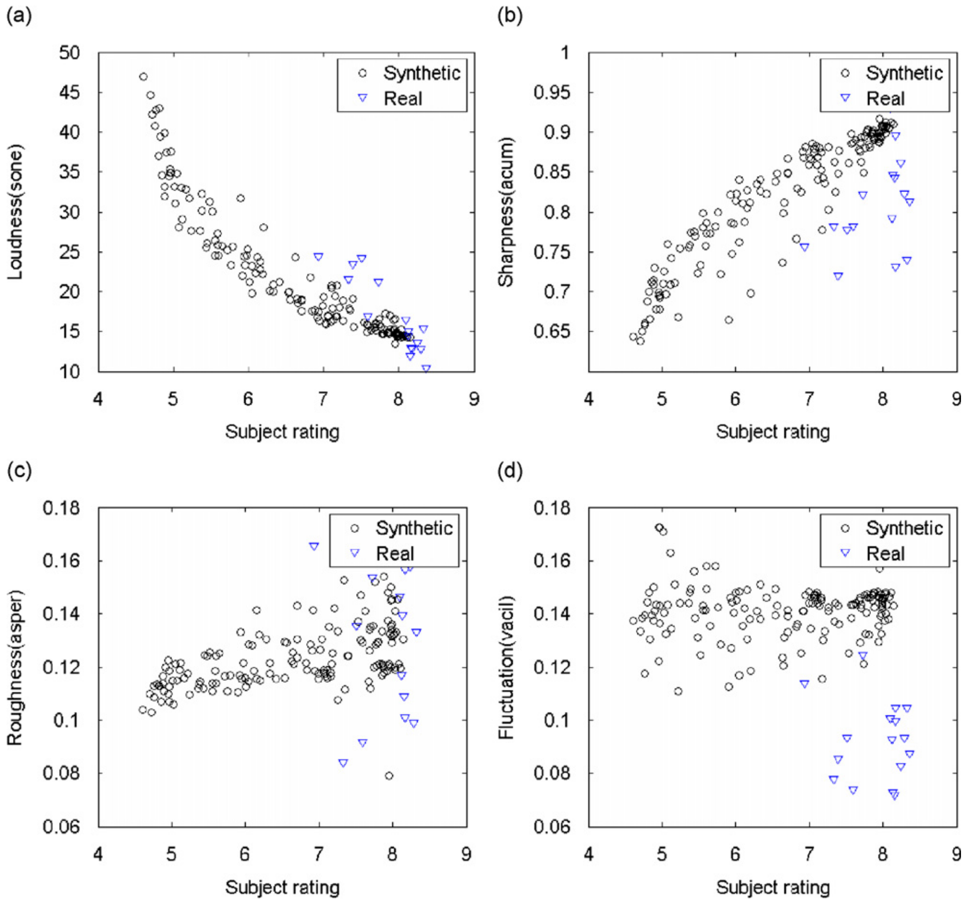

Fig. 11. Sound metric for the 166 interior sounds: (a) loudness for the signal filtered at 200 Hz frequency by lower pass filter using Zwicker's method, (b) sharpness for the 166 interior sounds of passenger cars using Bismarck's model, (c) roughness for the 166 interior sounds of passenger cars using Aures' model and (d) fluctuation strength for the 166 interior sounds of passenger cars using Fastl's model.

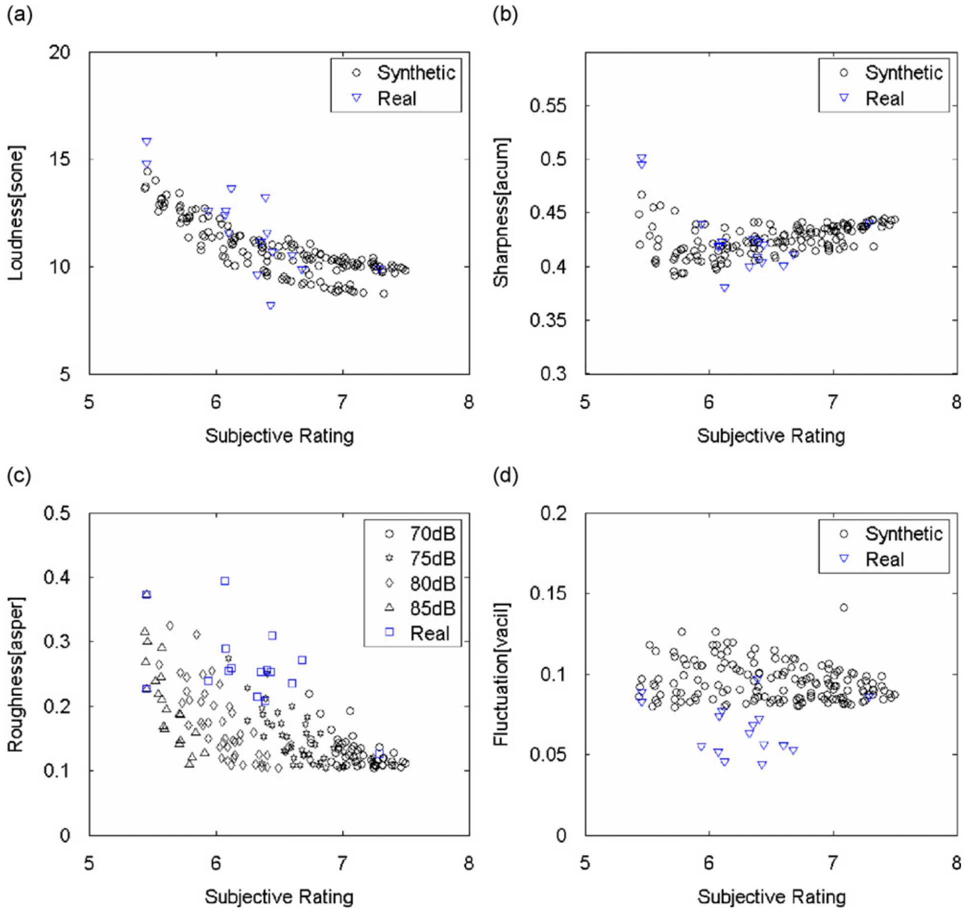

Fig. 12. Sound metric for the 166 interior sounds: (a) loudness for the signal filtered by 150–500 Hz frequency band filter using Zwicker's method, (b) sharpness for the 166 interior sounds of passenger cars using Bismarck's model, (c) roughness for the 166 interior sounds of passenger cars using Aures' model and (d) fluctuation strength for the 166 interior sounds of passenger cars using Fastl's model.

sound, the 166 interior sounds for rumbling sound are filtered by a band pass filter with frequency band between 200 and 500 Hz. From the graphic, the subjective ratio for both booming and rumbling sounds is proportional to 1/loudness.

6.2. Sharpness

Sharpness describes auditory perception related to the spectra correlation of a sound. Aures [26] and Bismarck [27] introduce the calculation model of sharpness. In this paper, Bismarck's model is also adopted for the calculation of sharpness for the 166 interior sounds. Sharpness is given by

$$S = 0.11 \times \frac{\int_0^{24} N' z g(z)\,\mathrm{d}z}{Nt}, \tag{22}$$

where N' is the specific loudness within the critical band (Bark) and $g(z)$ is a critical band rate-dependent weighting factor that is unity between 0 Bark and 16 Bark and then increases to four at 24 Bark. Nt is the total loudness. The unit of sharpness is acum. One acum is the sharpness for pure tone sound with an amplitude of 60 dB at 1 kHz. Fig. 11(b) shows the sharpness measured for the 166 sounds for booming sound. According to these results, the maximum sharpness is about 0.9 acum. At this level of sharpness, the subjective rate is about

8.2. From the graphic, it is concluded that the sharpness has a nonlinearly increasing relationship with human perception for the booming sound. The sharpness for interior sound of real passenger cars lies beneath these of synthetic interior sounds as shown in Fig. 11(b) since the background noise of real passenger cars is little different with that of synthetic sounds. Fig. 12(b) shows the sharpness measured for the 166 sounds for rumbling sound. According to these results, the maximum sharpness is about 0.5 acum. At this level of sharpness, the subjective rate is about 5.5. From the graphic, it is concluded that there is not a relationship between sharpness and human perception for rumbling sounds, since the change of sharpness does not induce a change of the subjective rate for rumbling sound as shown in Fig. 12(b).

6.3. Roughness

Roughness is the auditory perception character related to the amplitude modulation and frequency modulation for sound with frequency modulation at middle frequency around 70 Hz. It is related to the high-frequency modulation of the sound. Aures [28] introduced a calculation model of roughness for sound. The unit of roughness is the asper. One asper is the roughness for a pure tone sound with an amplitude of 60 dB at 1 kHz, which is 100% modulated in amplitude at a modulation frequency of 70 Hz. Fig. 11(c) shows the roughness measured for the 166 sounds for booming sound. According to these results, the maximum value of the roughness is about 0.18 asper. The change of roughness is not related the change for subjective rating. Fig. 12(c) shows the roughness measured for the 166 sounds for rumbling sound. From the graphic, it is difficult to conclude whether there is or is not a relationship between roughness and human perception for rumbling sounds, since the roughness has some hidden rule about the correlation with subjective rate. However, in psychoacoustics, the roughness is also related to amplitude modulation and frequency modulation. During acceleration, the sound wave in the compartment of a real car is an amplitude-phase-modulated signal. Therefore, the subjective rating for interior sound in a car should be related to the roughness. In order to find hidden rules, the subjective rate is plotted according to the magnitudes of the same carrier frequency components. From these results, it is found that the subjective rate is related to the magnitudes of the carrier frequency components. In Fig. 12(c), 70, 75, 80 and 85 dB mean the magnitude of the carrier frequency component, which is also the value of the A_j in Table 2. The magnitude of carrier frequency components is very closely related to the loudness. It is concluded that the subjective rating is proportional to 1/roughness when the magnitudes of the carrier frequency components are the same. Therefore, both sound metrics, loudness and roughness, have good correlation with rumbling sound.

6.4. Fluctuation strength

Fluctuation strength is the auditory perception character related to amplitude modulation and frequency modulation for sound with frequency modulation at lower frequency around 4 Hz. Zwicker and Fastl [13] proposed a calculation model of fluctuation strength for sound. The unit of fluctuation strength is the vacil. One vacil is the fluctuation strength for pure tone sound with an amplitude of 60 dB at 1 kHz, which is 100% modulated in amplitude at a modulation frequency of 4 Hz. Fig. 11(d) shows the fluctuation strength measured for the 166 sounds for booming sound. According to these results, the maximum value of fluctuation strength is about 0.18 vacil. It is also too small a value for humans to perceive the fluctuation strength for sound. From the graphic, it is concluded that the fluctuation strength has a slight relationship with human perception for booming sounds. Fig. 12(d) shows fluctuation strength measured for the 166 sounds for rumbling sound. From the graphic, it is again concluded that the fluctuation strength has a slight relationship with human perception for rumbling sounds. The fluctuation strengths for interior sound of real passenger cars lie beneath these of synthetic interior sounds as shown in Fig. 11(d) and 12(d) since the effect of frequency modulation at low frequency is over-estimated when the synthetic interior sounds are produced. However, these fluctuation strengths do not have a correlation with the subjective rating for booming sound and rumbling sound.

From the psychoacoustical analysis of the 166 interior sounds, not only is loudness for a signal filtered by a low pass filter very well related to subjective evaluation of booming sounds, but sharpness also has a relationship with it. Roughness and fluctuation strength are somewhat related. Therefore, low pass filtered loudness and sharpness are used for the input data of ANN. For rumbling sound, the loudness for signal filtered by a band pass filter with frequency band between 200 and 500 Hz and roughness is very well related to subjective evaluation of rumbling sounds. Therefore, band pass filtered loudness and roughness are used for the input data of ANN.

7. Sound quality index development

Recently, ANN has been applied to development of the annoyance index for the sound quality analysis of machinery [4,8,29,30]. In this paper, ANN is applied to development of the sound quality index of a passenger car. In the previous sections, the input and target for ANN were discussed. The type of ANN used in the paper is the multiple-layer network as shown in Fig. 3(b). The main work in this section is to find the optimal weights $w_{i,j}$ of connections. Basically, 150 interior sounds are synthesized and 16 interior sounds are obtained by measurement. Therefore, the averaged subjective rates for the 150 synthetic interior sounds are used for the target of the ANN being used for the sound quality index. Both loudness of lower frequency component and sharpness for 150 synthetic booming sounds and loudness of middle frequency component and roughness for 150 synthetic rumbling sounds are used for the input of the ANN. Therefore, the input of the ANN is a vector having elements of four sound metrics. The averaged subjective rates for booming sound and rumbling sound of the 150 interior sounds are used for the target of the ANN. The target of the ANN is a vector having elements of two subjective rates. The ANN being used as the sound quality index for a passenger car consists of 4–6–2 structure, i.e., $N = 4$, $H_1 = 6$ and $M = 2$. The number of weights in the connections for the input layer is 24. The number of weights of connects in the one hidden layer is 12.Optimal weights are obtained by training of the ANN.

Table 4 illustrates the optimal weights ($w_{i,j}$) of connects and threshold parameter (b_i) used at each layer. Mathematically, the sound quality index using these optimal weights of connect and threshold is written by

$$\text{Sound quality index} = F^2(\mathbf{LW}^2 F^1(\mathbf{IW}^1\mathbf{x} + \mathbf{b}^1) + \mathbf{b}^2), \tag{23}$$

where the function F follows the form of Eq. (3), $\mathbf{IW}^1$ is the weight matrix in the input layer, $\mathbf{LW}^2$ is the weight matrix of the first hidden layer. The output of the ANN is a vector with two elements which are the objectively estimated rates for booming sound and rumbling sound. Figs. 13 and 14 show the correlation between the output of the ANN and the averaged subjective rates. Fig. 13(a) shows the correlation between subjective rate for booming sounds and the first elements in the output vector of the ANN. It has a good correlation of 97.5%. Fig. 14(a) shows the correlation between subjective rate for rumbling sounds and the second elements in the output vector of the ANN. It has a good correlation of 96.5%.

In order to use the the trained ANN as the sound quality index, the trained ANN is tested with 16 interior sounds measured inside of 16 passenger cars. The loudness of lower frequency components, sharpness, loudness of middle frequency components and roughness for 16 interior sounds are used for the input of the trained ANN. Therefore, the input of the ANN is a vector having elements of four sound metrics. The output of the ANN is compared with the averaged subjective rate for the booming sound quality and rumbling sound quality. Fig. 13(b) shows the correlation between the subjective rate of booming sound quality for 16 interior sounds and the first elements in the output vector of the ANN. It has a good correlation of 93.2%. Fig. 14(b) shows the correlation between the subjective rate of rumbling sound quality for 16 interior sounds and the

Table 4
Weight function and bias for the sound quality index for a passenger car

Weights of input layer $\mathbf{IW}^1$				Weights of first hidden layer $\mathbf{LW}^2$		Bias of input layer $\mathbf{b}^1$	Bias of first hidden layer $\mathbf{b}^2$
3.1456	1.6296	0.4618	2.2758	−0.5533	−0.5850	1.3476	0.0986
0.8417	−0.7193	−1.0717	−3.5950	−0.4589	−0.2422	1.8540	0.2322
0.7270	−1.5875	1.0060	−1.1140	−0.1119	0.0841	−2.8243	
−0.3146	−0.3581	0.8095	0.0155	−0.9599	−1.4180	−0.1312	
−1.8049	−0.9006	5.8210	4.7802	0.0976	0.2507	−0.5676	
0.5130	4.5507	3.0081	−4.9321	−0.1599	−0.0782	−9.8306	

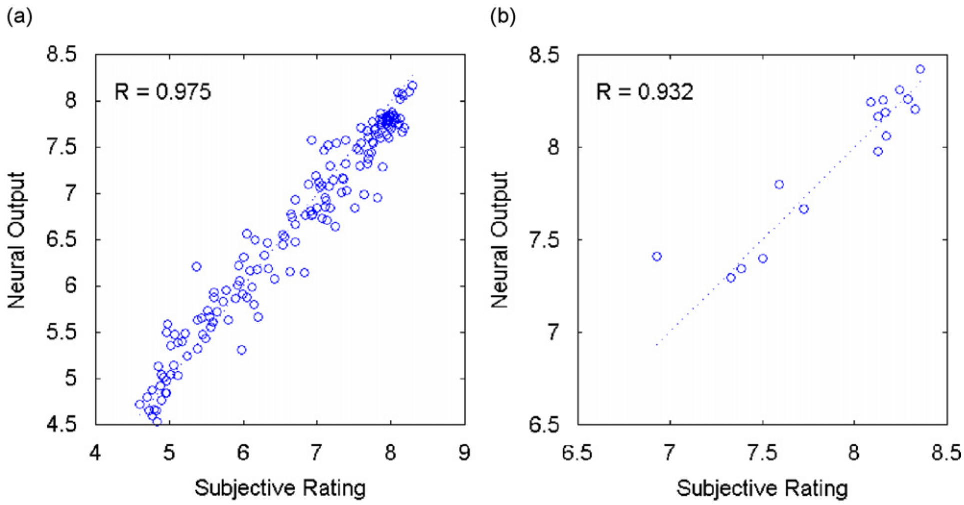

Fig. 13. Correlation between the output of the ANN and the averaged subjective rate (a) 166 synthetic booming sounds and (b) 16 interior sounds of passenger cars.

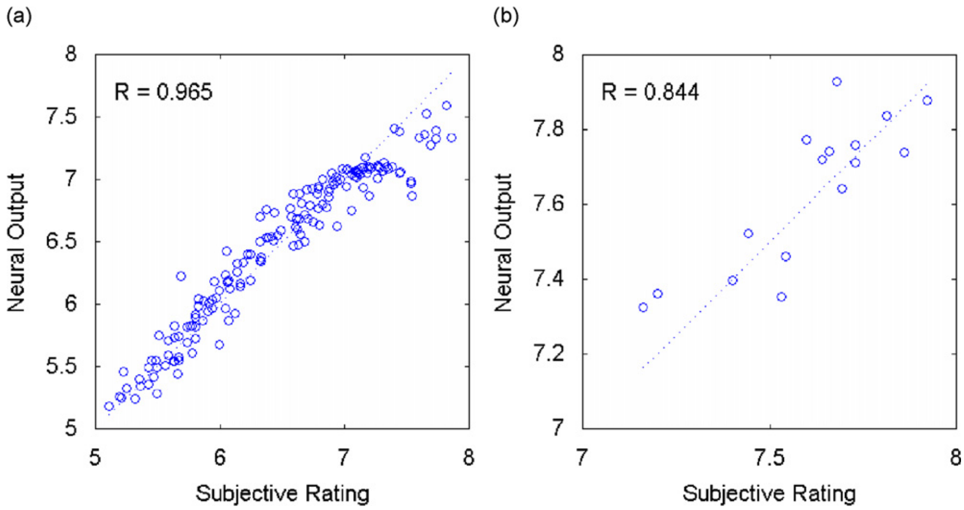

Fig. 14. Correlation between the output of the ANN and the averaged subjective rate: (a) 166 synthetic booming sounds and (b) 16 interior sounds of passenger cars.

second elements in the output vector of the ANN. It has a correlation of 84.4%. The correlation for the rumbling sound is not very high since among the 16 test cars used for the experiment, the 10 passenger cars are loaded with in-line 4-cylinder engines and the 6 passenger cars are loaded with V6 and V8 cylinder engines. In the previous work [8], the rumbling sound quality for a passenger car loaded with a v-type engine was more clearly heard inside the car than a passenger car loaded with an in-line type engine.

8. Application

The sound quality index for a passenger car developed by using the ANN was applied to the enhancement of the interior sound quality of a passenger car. For application, the interior sound for 20 competitive mass-produced passenger cars was measured and their sound quality was estimated objectively by using the developed ANN in the previous section. The four sound metrics for the 20 interior sounds are calculated. For the booming sound quality, low pass filtered loudness and sharpness are calculated, and for the rumbling sound quality, band pass filtered loudness and roughness are calculated. By inserting these four sound metrics into Eq. (23), the objective rates of the booming sound quality and rumbling sound quality for 20 interior sounds can be obtained and plotted in the sound metrics space. Fig. 15 shows the contour map for the objective rates of booming sound quality in the space of two sound metrics, which are low pass loudness and sharpness. According to these results, when the low pass loudness is over 12 sones, the booming rate goes down linearly. In order to get high point booming rate, the sharpness should also be considered. Fig. 16 shows the contour map for the objective rates of rumbling sound quality in the space of two sound metrics, which are band pass loudness and roughness. According to these results, in order to get the high point rumbling rate, both the loudness and roughness should be low simultaneously.

Until now, the booming sound quality and rumbling sound quality have been objectively estimated by the sound quality index, which is developed by ANN. However, in order to estimate the preference for the interior sounds of the passenger cars, the booming level and rumbling level for 20 interior sounds should be considered simultaneously. Therefore, the output of the ANN for 20 interior sounds is plotted in the two-dimensional spaces of rumbling level and booming level. In addition, the interior sounds for two developmental passenger cars are measured. The output of the ANN for these two sounds is also plotted in the same space as shown in

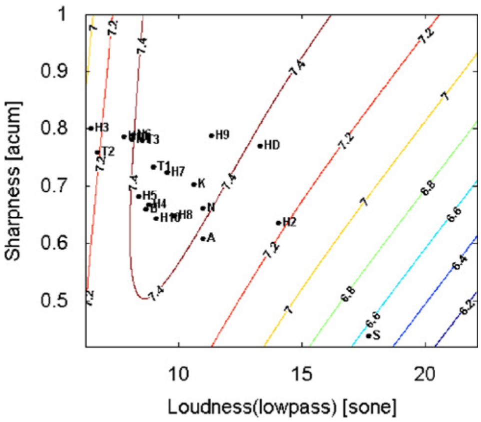

Fig. 15. Contour map of booming index for the sound metrics having high correlation with the booming index (HD = Honda, B = BMW, K = KIA, H = Hyundai, T = Toyoda, S = Samsung, N = Nissan).

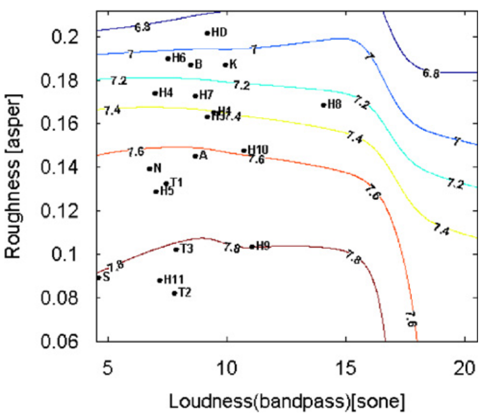

Fig. 16. Contour map of rumbling index for the sound metrics having high correlation with the booming index (HD = Honda, B = BMW, K = KIA, H = Hyundai, T = Toyoda, S = Samsung, N = Nissan).

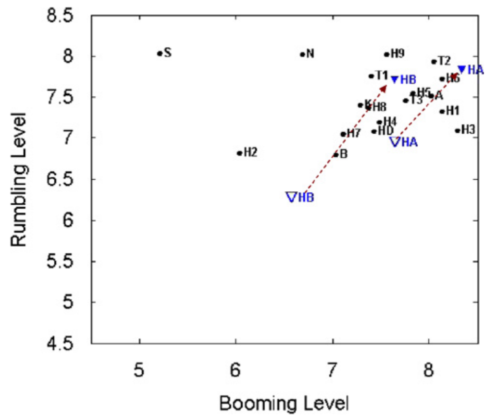

Fig. 17. Contour map for the interior sound of passenger cars during acceleration in view of booming sound and rumbling sound (HD = Honda, B = BMW, K = KIA, H = Hyundai, T = Toyoda, S = Samsung, N = Nissan, HA = Hyundai Type A, HB = Hyundai Type B, ▼ = mass production car, ▽ = prototype car).

Fig. 17. In Fig. 17, the booming rate and rumbling rate of two developmental cars are marked as "HA" and "HB". The "HA" and "HB" mean passenger car A and passenger car B being developed at the Hyundai Motor Co., respectively. From this result, it is concluded that the booming rate and rumbling of two developmental passenger cars are enhanced during the development period from prototype state to mass production state. The sound quality index is usefully applied to the development of sound quality of a passenger car during acceleration.

9. Conclusions

An ANN has been applied to the development of the sound quality index of the booming sound and rumbling sound of passenger cars. A total of 150 synthetic signals are used for the training of ANN, and the interior sounds of 16 mass-produced passenger cars are used for the confirmation of the trained ANN. The structure of the ANN used in the present paper is a back-propagation neural network with 4–6–2 structure. The input vector of the ANN has four elements and the output vector has two elements. The average subjective rates for the 150 synthetic interior sounds are used for the target of the ANN being used for booming index and rumbling index. The subjective rates for 150 synthetic sounds and 16 interior sounds measured inside cars were evaluated by 21 passengers.

It is found that the loudness filtered by a low pass filter and sharpness have a strong relationship with the average subjective rates of booming sounds, and that loudness filtered by band pass filter and roughness have a strong relationship with the average subjective rates of rumbling. Therefore, loudness with low-frequency component, loudness with middle frequency component, sharpness and roughness for those interior sounds are calculated for the input of the ANN.

The correlations between the output of the ANN and the average subjective rate for 150 booming sounds and rumbling sounds are 97.5% and 96.5%, respectively. It is concluded that the output of the trained ANN can be used for the sound quality index for the interior sounds of passenger cars. This has been confirmed with the application of the trained ANN to the estimation of the subjective rates for the sound qualities of the interior sounds of 16 passenger cars. The output of the trained ANN has 93.2% correlation for booming sound and 84.4% correlation for rumbling sound with the average subjective rates evaluated by 21 passengers. For application of the sound quality index to the practical development of the interior sound quality for passenger cars, the sound quality of 20 competitive passenger cars was estimated with the trained ANN and their level was plotted in the two spaces of booming level and rumbling level. The sound quality of two developmental cars is enhanced and their results are also confirmed in the two-dimensional spaces of booming level and rumbling level.

Acknowledgments

This work was supported by INHA UNIVERSITY Research Grant.

References

[1] S. Matsuyama, S. Maruyama, Booming noise analysis method based on acoustic excitation test, *Proceeding of the SAE 1998 World Congress and Exhibition*, March 1998, Detroit, Michigan, USA, SAE980588.

[2] S. Hatano, T. Hashimoto, Booming index as a measure for evaluating booming sensation, *Proceedings of Inter-Noise 2000*, July 2000, Nice, France, CD-ROM Reference Number 000233.

[3] Murata, H. Tanaka, H. Takada, Y. Ohsasa, Sound quality evaluation of passenger vehicle interior noise, *Proceedings of the 1993 SAE Noise and Vibration Conference*, May 1993, Traverse City, Michigan, USA, SAE931347.

[4] S.K. Lee, H.C. Chae, D.C. Park, S.G. Jung, Sound quality index development for the booming noise of automotive sound using artificial neural network information theory, *Sound Quality Symposium 2002*, August 2002, Dearborn, Michigan USA, CD N0.5.

[5] K. Tsuge, K. Kanamaru, T. Kido, N. Masuda, A study of noise in vehicle passenger compartment during acceleration, *Proceedings of the SAE 1998 World Congress and Exhibition*, March 1998, Detroit, Michigan, USA, SAE980965.

[6] T. Wakita, Y. Kozawa, K. Samada, G. Sugimoto, T. Ogasawara, Objective rating of rumbling in vehicle passenger compartment during acceleration, *Proceedings of the 1998 SAE Noise and Vibration Conference*, May 1998, Traverse City, Michigan, USA, SAE891155.

[7] M. Croker, M. Maunderm, Reducing crank rumble using transfer path analysis to assess engine modifications, *Proceedings of the 2003 SAE Noise and Vibration Conference*, May 2003, Traverse City, Michigan, USA, SAE2003-01-1428.

[8] S.K. Lee, B.Y. Kim, H.C. Chae, D.K. Park, S.G. Jung, Sound quality analysis of a passenger car based on rumbling index, *Proceedings of the 2005 SAE Noise and Vibration Conference*, May 15–18, 2005, Traverse City, Michigan, USA, SAE2005-01-2481.

[9] A. Gonzalez, M. Ferrer, M. de. Diego, G. Pińero, J.J. Garcia-Bonito, Sound quality of low-frequency and car engine noise after active noise control, *Journal of Sound and Vibration* 265 (2003) 663–679.

[10] D. Vastfjall, M.A. Gulbol, M. Klieiner, T. Garling, Affective evaluation of reactions to exterior and interior vehicle auditory quality, *Journal of Sound and Vibration* 255 (3) (2002) 501–518.

[11] S. Namba, S. Kuwano, A. Kinoshita, Hayakawa, Psychological evaluation of noise in passenger cars- The effect of visual monitoring and the measurement of habituation, *Journal of Sound and Vibration* 205 (4) (1997) 427–433.

[12] S. Blommer, S. Amman, S. Abhyankar, B. Dedeker, Sound quality metric development for wind buffeting and gusting noise, *Proceedings of the 2003 SAE Noise and Vibration Conference*, May 2003, Traverse City, Michigan, USA, SAE2003-01-1509.

[13] E. Zwicker, H. Fastl, *Psychoacoustics: Facts and Models*, second ed., Springer, Berlin, 1999.

[14] Q.Z. Zhang, X.D. Li, W.S. Gan, Active noise control using a simplified fuzzy neural network, *Journal of Sound and Vibration* 272 (2004) 437–449.

[15] Y.L. Zhou, Q.Z. Zhang, X.D. Li, W.S. Gan, Analysis and DSP implement of an ANC system using a filtered-error neural network, *Journal of Sound and Vibration* 285 (2005) 1–25.

[16] S. Tomasiello, An application of neural networks to a non-linear dynamics problem, *Journal of Sound and Vibration* 272 (2004) 461–467.

[17] P.Q. Xia, An inverse model of MR damper using optimal neural network and system identification, *Journal of Sound and Vibration* 266 (2003) 1009–1023.

[18] C.M. Bishop, *Neural Networks for Pattern Recognition*, Oxford University Press, London, 1995.

[19] H. Matrn, *Neural Network Design*, PWS, Publishing Company, London, 1996.

[20] K. Lee, Adaptive Signal Processing and Higher Order Time Frequency Analysis for Acoustic and Vibration Signatures in Condition Monitoring, PhD Thesis, Institute of Sound and Vibration Research, University of Southampton, UK, 1998.

[21] S.K. Lee, P.R. White, The enhancement of impulsive noise and vibration signals for fault detection in rotating and reciprocating machinery, *Journal of Sound and Vibration* 217 (3) (1998) 485–505.

[22] G.H. Herlufsen, H.K. Hansen, H. Vold, Characteristics of the Vold–Kalman order tracking filter, *Bruel & Kjaer Technical Review* (1998).

[23] S.A. Andrews, D. Anderton, The analysis and mechanism of engine crank rumble, *Proceedings of the Institution of Mechanical Engineers* (1979) 99–109.

[24] S.S. Stevens, Perceived level of noise by MarkII and decibels, *The Journal of the Acoustic Society of America* 51 (1971) 575–601.

[25] B.C.J. Moore, B.R. Glasberg, A revision of Zwicker's loudness model, *Acoustica* 82 (1996) 335–345.

[26] W. Aures, A procedure for calculating auditory roughness, *Acoustica* 58 (1985) 268–281.

[27] V. Bismarck, Sharpness as an attribute of the timbre of steady sounds, *Acoustica* 30 (1974) 159–172.

[28] W. Aures, The sensory euphony as a function of auditory sensations, *Acoustica* 58 (1985) 282–290.

[29] P.C. Laux, Using Artificial Neural Networks to Model the Human Annoyance to Sound, PhD Thesis, School of Mechanical Engineering, Purdue University, USA, 1998.

[30] H.U. Prante, Estimation of sound quality measures using FIR neural network, *Acoustica* 85 (1999) 674–677.